Building Tomorrow's Society
Bâtir la Société de Demain

Fredericton, Canada
June 13 – June 16, 2018/ *Juin 13 – Juin 16, 2018*

AN ALTERNATIVE INTERPRETATION OF ONE-WAY SHEAR STRENGTH: STRAIN PENETRATION IN LONGITUDINAL BAR ANCHORAGE

Eshghi, Najmeh[1,3] and Pantazopoulou, S.J.[2]
[1] MSc Candidate, Department of Civil Engineering, York University, Canada
[2] Professor of Civil Eng., Lassonde Faculty of Engineering, York University, Canada, pantazo@yorku.ca
[3] neshghi@yorku.ca

Abstract: Significant effort has been vested over the years in quantifying the contribution of concrete to the shear strength of RC members. Design code expressions have been calibrated to a carefully assembled database of tests, where success of each design proposal is tested from its concurrence with the experimental sensitivities for the range of the design parameters, including size-related phenomena which are attributed to the brittle fracture of concrete. Recent advances in the study of bond and anchorage have provided insights into a totally new interpretation of shear failure. It is shown that strain penetration over the unconfined length, which spreads further into the anchorage with increasing moment at midspan, may propagate over the entire length of available longitudinal reinforcement, perpetrating brittle failure and collapse at loads that are much lower than the nominal shear strength. With this approach it is possible to reproduce successfully the experimental trends and to provide an alternative interpretation to the size effect which seems to be owing to the reduced bond strength of larger size bars in unconfined anchorages and the need for longer anchorage lengths - parameters that have not been accounted for in the past when calibrating shear models with test results. Examples from the experimental database of ACI 445 are solved using the mechanistic model for strain penetration in the shear span of a loaded beam; analytical estimates are calibrated against the test values. The significance of the work lies in the prospect it offers for a totally different look at shear design and the determination of the V_c term for practical applications.

1 INTRODUCTION

The debate about the contribution of concrete term to the shear strength of prismatic Reinforced Concrete (RC) members has been ongoing for at least 40 years and recently it has been refueled on the occasion of revision of the technical guideline of ACI-ASCE Committee 445 (referred to hereon as C445) (Belarbi et al. 2017). For reasons of simplicity and clarity, expressions estimating the concrete contribution term V_c have been developed with reference to the shear strength of concrete beams without transverse reinforcement. The debate reflects the uncertainty about the role of the crucial variables affecting V_c : experiments indicate that the shear strength of concrete members does not increase proportionately with the bearing (web) area, $b_w d$ – but that instead, there is an implicit size-effect in V_c that is owing to fracture mechanics considerations (Bazant and Planas 1997) and the larger aggregate size used in real life members as compared to the specimens tested in laboratories (Collins and Kuchma 1999). Revisiting this problem is one more attempt by ACI-ASCE 445 to correct the discrepancies between test results and design expressions.

About 20 years ago, C445 established a carefully controlled database of hundreds of concrete beam tests (Reineck et al. 2003, Belarbi et al. 2017). The database has been used to refine a variety of empirical design expressions and models for V_c; acceptance criterion is the ability of the design model to reproduce the experimental sensitivities over the entire range of the experimental parameters. It was already known

that empirical models for shear performed adequately when used for beams having similar sizes as those used for model calibration; however significant deviations were observed between calibrated models and test results outside the range of parameters studied, the most dramatic being a systematic overestimation of beam strengths with larger than common size. This became known as "the size effect in shear" and it has been at the center of the shear controversy for years (Kani 1967, Ozbolt and Eligehausen 1995, Collins and Kuchma 1999, Bažant 1999, Karihaloo et al. 2003, Cladera and Marí 2004, Grégoire and Laboratoire 2013, Kirane et al. 2016, Belarbi, Kuchma, and Sanders 2017). Reineck et al. (2003) assessed the ACI 318-14 design expression for V_c using the database, concluding that the ACI 318-14 provisions for shear strength of beams without stirrups becomes increasingly unsafe "as members become larger and more lightly reinforced."

In fact, simple comparison between the experimental values for shear strengths of beams without any stirrups (V_{test}) in the database with the values calculated as per ACI 318-14 (V_{ACI}) demonstrates significant scatter particularly in the case of larger members (Fig. 1). This underscores the fact that the true mechanism behind the shear failure is not completely understood and there might be important aspects that are overlooked in the established models. This observation motivated the initiative of C445 to address the discrepancies between experimental shear values and analytical estimates. So, in 2014, a campaign was undertaken to collect and evaluate new proposals for safer and more reliable design models for the shear strength of concrete beams. Litmus test for acceptance of any proposal was its performance against the C445 database. A total of 10 proposals were submitted which were eventually reduced to six, as listed in Table 1 along with the current (ACI 318-14) design expression for the "concrete contribution to shear strength", V_{ACI}.

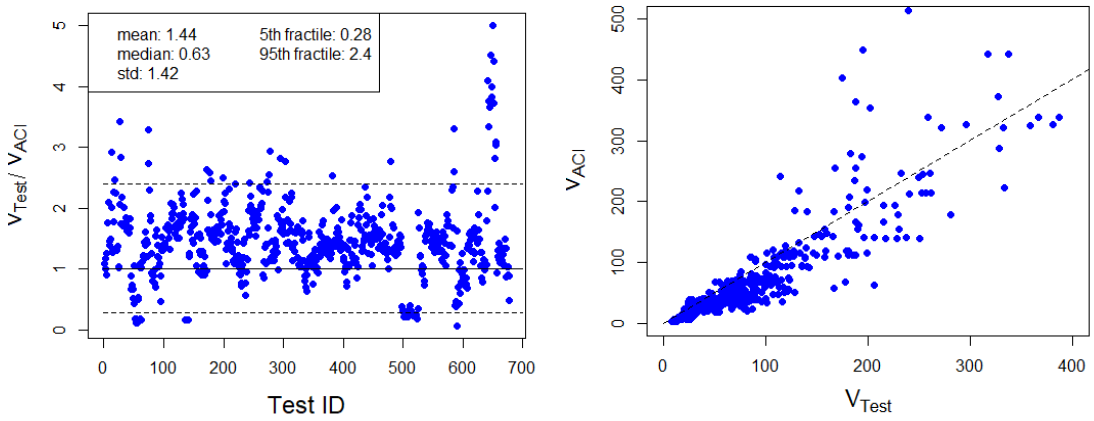

Figure 1: (a) Measured V_c value normalized with respect to V_{ACI}; (b) V_c plotted against V_{ACI}: note that discrepancy increases in the range of larger forces measured (i.e. in larger beams)

Table1: Competing Design Expressions for V_c after the recent campaign by C445*

Proposal ID	Concrete contribution to shear strength, $\boldsymbol{V_c}$
ACI 318-14	$V_c = 2\lambda\sqrt{f_c'}\,b_w d$
(Bentz and Collins 2017) (for beams without stirrups and 3/4 in. aggregate size)	$V_c = \frac{100}{38 + s_x}\sqrt{f_c'}\,b_w d$ $s_x = 0.9\,d$
(Cladera et al. 2017) *(note: the limit on c/d proposed by the authors has been neglected because it yielded unrealistic strength estimates)*	$V_c = 6\lambda\xi\frac{c}{d}\sqrt{f_c'}\,b_{v,eff}d < 4\left(1.25\xi\frac{c}{d} + \frac{1}{d_0}\right)\sqrt{f_c'}\,b_w d$ $\xi = \frac{2}{\sqrt{1+{d_0}/{8}}}\left(\frac{d}{a}\right)^{0.2};\ a = \frac{M_{u,max}}{V_{u,max}};\ d_0 = \max\{d, 4in\};$

	$\frac{c}{d} = 0.75\,(n\rho)^{1/3}$
(Frosch et al. 2017)	$V_c = \left(5\lambda\sqrt{f_c'}\ b_w c\right)\gamma_d$ $c = d(\sqrt{2\rho n + (\rho n)^2} - \rho n)\ \ c = kd\ \ ;\ \ \rho = \frac{A_s}{b_w d}\ \ ;\ \ n = \frac{E_s}{E_c}\ ;$ $\gamma_d = 1.4/\sqrt{1 + {}^{d_t}/_{10}}$
(Li et al. 2017)	$V_c = 17\lambda\left(\frac{V_u d}{M_u}\right)^{0.7} \cdot \sqrt{f_c'}\ b_w c \cdot \frac{1}{\sqrt{1 + {}^{h}/_{11.8}}} < 10\lambda\sqrt{f_c'}\ b_w c$ $c = d\left(\sqrt{2\rho n + (\rho n)^2} - \rho n\right)\ ;\ \rho = \frac{A_s}{b_w d}\ \ ;\ \ n = \frac{E_s}{E_c}$
(Park and Choi 2017)	$V_c = k_s f_t b_w c\ cot\phi$ $k_s = \left(\frac{12}{d}\right)^{0.25} < 1.1\ \ \ ;\ \ f_t = 2.2\lambda\sqrt{f_c'}\,;$ $cot\phi = \sqrt{1 + {}^{\sigma_{ct}}/_{f_t}}\ ;\ \sigma_{ct} = \frac{M_u}{b_w c\,(jd)}$
(Reineck 2017)	$V_c = \phi\left[71\,\eta\left(\rho\,\frac{f_c'}{d}\right)^{1/3}\right] b_w\,d \qquad \rho = \frac{A_s}{b_w\,d}$

* *All equations are in U.S customary units (psi, in). $b_{v,eff}$ is the effective section width for shear strength; c is the neutral axis depth; d_t is the distance in inches from the extreme compression fiber of the member to the centroid of the reinforcement nearest the tension face; η and λ are modification factors for lightweight concrete;*

The concern regarding "size effect" in concrete beams (i.e. the disproportional increase of shear strength and beam depth) is reflected in the models by introducing what is considered the most critical variable in determining shear strength, i.e., the shear span-to-effective depth. By inspection of the proposed equations, it may be seen that longitudinal reinforcement is only considered as a ratio (percent) over the cross section, to the extent that it controls the depth of compression zone, c. Note that the underlying assumption of those models where V_c depends on c is that shear transfer in concrete only occurs over the depth of compression zone. Therefore, none of the proposals makes any reference to longitudinal bar size and its implications on the state of bond along the reinforcement, which however is essential for the composite action of the beam. Evidently several of the parameters that affect the concrete-reinforcement interaction, such as bar size, cover, and development length, have been neglected in the emerging shear strength proposals. The significance of the effect of bar size is illustrated clearly in experimental test results presented by Taylor (1972) and Daluga et al. (2017). While other researchers reported up to 68% reduction of mean unit shear strength by increase of section depth from 12 to 36 in. (305 to 914mm), Daluga et al. (2017) claimed that the reduction is much smaller (14%) for beam depth from 12 to 48in. (305 to 1219mm) and it is even smaller than the statistical error of experimental data. It is worth noting here, that size effect is explicitly recognized in bond research (fib bulletin 72, 2014): Larger bar sizes have lower bond strength, whereas cover splitting, and anchorage length are not proportional to the bar size (fib Model Code 2010):

[1] $f_{b,0} = \eta_1\eta_2\eta_3\eta_4(\frac{f_{ck}}{20})^{0.5}/\gamma_c\ ;$

where, $f_{b,0}$ is the design bond strength; f_{ck} is the characteristic cylinder concrete compressive strength; η_1 accounts for the bar profile (η_1*=1.8* for ribbed vs. η_1*=0.9* smooth); η_2 accounts for the "top bar" effect (*=1* in the absence of top bar effect); η_3 accounts for the bar diameter effect (*=1* for $D_b \leq 20mm$, $\eta_3 = (20/D_b)^{0.3}$ for $D_b > 20mm$); η_4 accounts for the characteristic strength of steel reinforcement (*=1.2, 1.0,* and *0.85* for f_y*=400, 500* and *500 MPa* respectively), and γ_c is the material safety factor (*=1.5*). The ultimate bond strength, f_{bd}, is obtained also considering the effect of confinement:

[2] $f_{bd} = (\alpha_2 + \alpha_3) f_{b,0} + 2p_{tr} < 2f_{b,0} + 0.4p_{tr} < 2.5\sqrt{f_{ck}}$

where α_2, α_3 represent the influence of passive confinement from cover and from transverse reinforcement, respectively, and p_{tr} is the transverse pressure.

The concept that shear failure of beams without stirrups may be an indirect manifestation of bond failure is pursued in the present paper. Considering the mechanics of bond, development of bar stresses in the shear span (i.e. over the length in which the applied moment decays from its peak value to zero) is calculated. It is shown that the governing mechanism behind the failure of many tests that are treated in the C445 database as shear failures are in fact bond failures along the longitudinal reinforcement which is very much affected by the bar size. Therefore, the problem referred to "size effect" in shear, is in fact much more related to the scaling of the bar size.

Recently, the solution of the governing equations of bond of a bar developed under a moment gradient was established (Megaloeconomou et al. 2017). It was shown that a disturbed region forms near a flexural/shear crack, whereby the stresses in the reinforcing bar cannot be obtained from flexural analysis considering the moment acting in the cross section of interest, but rather, stresses are controlled by the solution of the bond equation. As the flexural moment in critical section increases, the disturbed region spreads towards the support and the end of the bar anchorage. This process is referred to as strain penetration. Before, inelastic strain penetration in the anchorage of a reinforcing bar had already been established (Tastani and Pantazopoulou 2013a, 2013b). Megalooikonomou et al. 2018 used this solution to determine the plastic hinge length in the shear span of a laterally swaying column.

In the present paper a consistent definition of shear failure and the corresponding strength of the failure mechanism is pursued with reference to the actual state of bond of reinforcement along the shear span of a beam. First, localization of each new flexural crack is evaluated. Location of primary flexural cracks is the starting point for calculating the disturbed region and for monitoring its propagation with increasing load. The last possible flexural crack location is critical, and it depends on the ratio of M_{cr}/M_{max} . If the residual development length from the last crack to the bar end is not sufficient to develop the bar force demand, bond failure will occur, manifested by splitting along the anchorage towards the bar end, and accompanied by beam failure, generally at a load that is much lower than the beam shear strength (Fig. 2). The following section summarizes the analytical steps of this derivation.

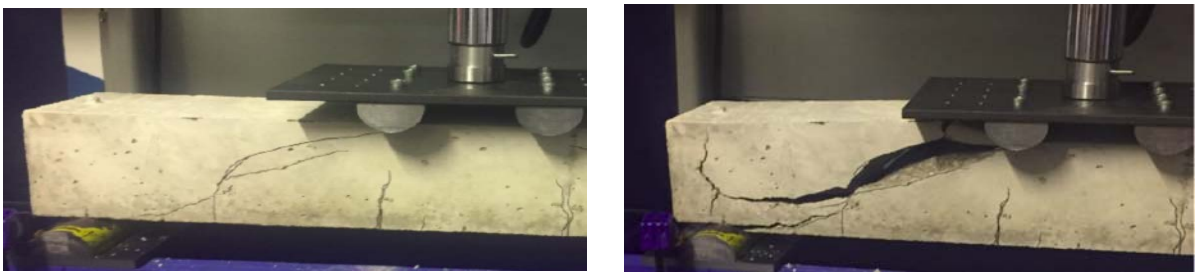

(a) (b)

Figure 2: Failure patterns in a beam without stirrups with longitudinal 3-10M bars at the onset of shear cracking (a) and at failure (b).

2 STATE OF STRESS IN SHEAR SPAN OF A BEAM

The moment distribution along the shear span of a beam, of length L_s, (Fig. 3) follows Eq. 3a:

[3a] $M(x) = M_0 (1 - {}^{x}/_{L_s})$

Before cracking, the strain in the bar and concrete at the level of the reinforcement, $\varepsilon_{fl}(x)$, is given by Eq. 3b, where y_g is the distance of the reinforcement from the centroid of the cross section. With increasing load, and when peak moment at midspan exceeds the cracking moment M_{cr}, the first crack occurs in the

critical region, usually under the point load; this location is used as point of reference hereon, and therefore $x_{cr1} = 0$ (i.e., first crack at x_{cr1}). From flexural analysis, bar stain is estimated from:

[3b] $\varepsilon_{fl}(x) = M\,(x).\ y_g/E_c.I_g$

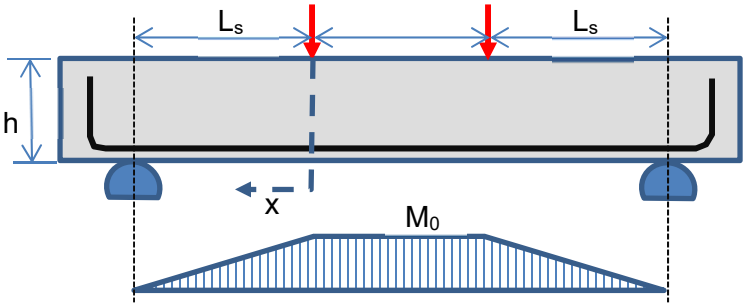

Figure 3: Moment distribution along the length of a beam: L_s is the shear span

Upon fist crack formation, the effective section stiffness is reduced drastically (e.g. 1/3 of uncracked stiffness). Therefore, with an imperceptible increase of moment at the critical section to $M_{cr} + \delta$ the bar strain experiences a significant jump in order to maintain equilibrium. At the crack, the concrete strain at the bar level reduces to zero due to cracking whereas the reinforcement strain increases dramatically to $\varepsilon_{so}\ (x = 0)$, where it is assumed that the post-cracking relationship between flexural moment, curvature and bar strain has been computed from classical sectional analysis of the critical section. Once the compatibility between bar and concrete normal strain is violated by cracking, it ceases to be valid over a distance, l_{D1}, away from the crack. The distance, referred to as "disturbed region", l_{D1}, is a necessary development length for bar stresses before concrete may be fully engaged again through bond. Thus, Eq. 3b is no longer valid over l_{D1}. Instead, the bar strain is calculated over l_{D1} from bond. Note that the governing equations that describe the transfer of force from bar to the surrounding concrete cover, and the corresponding compatibility between bar slip s, concrete strain,ε_c, and bar strain, ε_s, are as follows:

[4a] $\frac{df}{dx} = \left(-\frac{4}{D_b}\right) f_b$

[4b] $\frac{ds}{dx} = -(\varepsilon_s - \varepsilon_c) = -\varepsilon_s$ (Here it is assumed that ε_c is negligible in comparison with ε_s).

Considering the stress-strain and bond-slip relationships for the reinforcement (ascending branch in Fig. 4): $f_s = f_s(\varepsilon_s)$ and $f_b = f_b\,(s)$, the bar strain, $\varepsilon_s(x)$, may be calculated for segment l_d from solution of Eq. 4a and Eq. 4b. Here, the reinforcing bar stress-strain relationship, $f_s(\varepsilon_s)$, is considered elastic-plastic with hardening (Fig. 4a) whereas the local bond-slip relationship $f_b\,(s)$ is assumed to be a linear elastic, perfectly plastic curve with zero residual bond (Fig. 4b). Upon substitution in Eq. 4a and Eq. 4b of the ascending linear equations of $f_s(\varepsilon_s)$ and $f_b\,(s)$ the following differential equation of bond is obtained (Eq. 5):

[5] $\frac{d^2\varepsilon_s}{dx^2} = \left(-\frac{4f_b^{max}}{s_1 E_s D_b}\right)$

which is solved for the bar strain, $\varepsilon_s\,(x)$, over l_{D1}:

[6] $\varepsilon_s(x) = C_1 e^{-\omega x} + C_2 e^{\omega x}$, where, $\omega = \sqrt{4f_b^{max}/E_s\ D_b s_1}$

Thus, if slip remains below the value of s_1, (Fig. 4(b)) over the disturbed length, l_{D1}, the reinforcement strain is calculated by the solution of the bond equation. The end of the disturbed length l_{D1} is defined by the requirement that the bar strains obtained at $x = l_{D1}$ from bond (Eq. 6) and from flexural action (Eq. 3) converge – so that at $x = l_{D1}$ the bar strain compatibility with the surrounding concrete cover is satisfied. This is expressed by the boundary conditions given by Eq. 7 and 8. For this stage, the following conditions are solved for calculating l_{D1} :

1) Slope of the strain distribution obtained from bond solution and flexure are equal:

[7] $\omega\,(-C_1 e^{-\omega l_{D1}} + C_2 e^{\omega l_{D1}}) = M_0.\ y_g / E_c.I_g.L_s$

2) Bar strain calculated from Eq. 6 and Eq. 3b are equal:

[8] $C_1 e^{-\omega l_{D1}} + C_2 e^{\omega l_{D1}} = \frac{M_0.\ y_g}{E_c.I_g}(1 - {}^{l_{D1}}/_{L_s})$

In order to develop a step by step algorithm for the solution, the tension strain ε_{s0} at the critical cross section is chosen as the controlling variable; therefore at $x = 0$, the solution of the bond equation leads to:

[9] $\varepsilon_s\,(x = 0) = C_1 + C_2 = \varepsilon_{s0}$

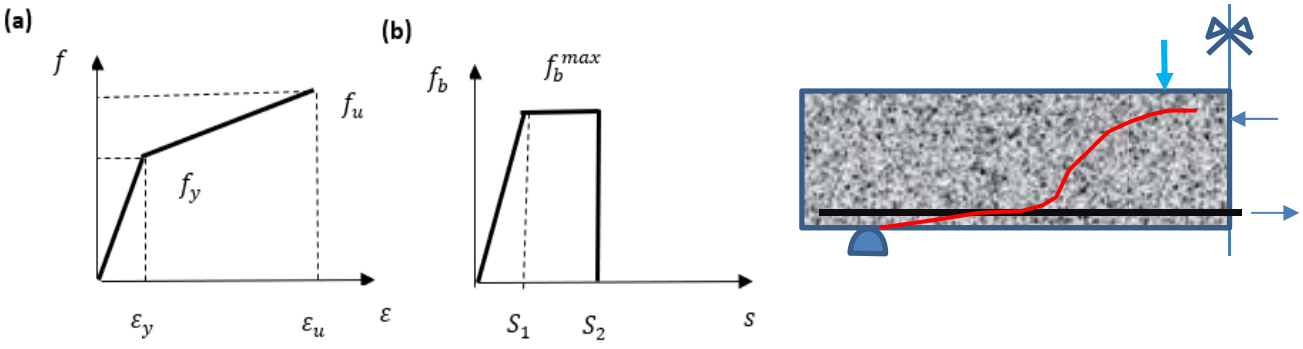

Figure 4: (a) General stress strain diagram for steel and (b) bond-slip relationship; (c) Common shear failure crack pattern of beams without stirrups

Equations 7, 8, and 9 have three unknowns, i.e., C_1 , C_2 , l_{D1}. The system is solved step by step, for any value of the controlling variable, ε_{s0}, in order to define the distribution of bar strains, slip values and the length of disturbed region, l_{D1}. The next crack is at $x_{cr,2}$: the crack may be either inside l_{D1} (governed by bond equation) or it may happen in the undisturbed region and will be evaluated based on the flexural theory. Specifically, if the next crack occurs:

a) inside the disturbed region: In this case, $x_{cr,2}$ can be found if the force transferred through bond to the concrete cover exceeds the tensile resistance of the effective area of concrete cover engaged in tension:

[10] $E_s A_{s1}(\varepsilon_0 - \varepsilon(x)) > f_{ct} A_{c,eff}$ where $A_{c,eff} = b\,(2C_{cov} + D_b) - A_{s1}$

b) in the undisturbed region: Here, $x_{cr,2}$ is calculated from the following equation.

[11] $\varepsilon(x_{cr,2}) = \frac{M_0.\ y_g}{E_c.I_g}\left(1 - {}^{x_{cr,2}}/_{L_s}\right) = \varepsilon_{c,cr}$

After localization of the second crack, the new disturbed region, l_{D2}, which extends from the second crack location, $x_{cr,2}$, is calculated. The process is repeated until no additional primary cracks can form as the moment increases: this stage is known as crack stabilization. From this stage on, until failure, the anchorage solution is used over the entire length, L_b, which is measured from the critical section to the end of the bar length (so the boundary condition in that stage is, $\varepsilon(L_b) = 0$).

Failure occurs when either (a) ε_{s0} exhausts the ultimate strain of the M-ε diagram, or (b) the total length L_D exceeds the available development length of the bar in the shear span, taken here as $L_s + h_{hook}$. After creation of the last primary crack, it is necessary to check whether the bar force required for flexure at the last crack, $(A_s E_s \varepsilon_{s,cr})$ can be equilibrated by the bond force along the available development length of the bar, to be evaluated from the bond solution. If the remaining length is shorter than expected to carry the bar force through bond, failure will occur by splitting along the bar.

3 ACCOUNTING FOR BOUNDARY CONDITIONS

Tests are conducted with different construction details which may create different boundary conditions to the problem stated above. In order to approximate the distribution of bar strains over the disturbed length along the shear span, the proper boundary conditions should be selected. For example, if the tension reinforcement is anchored properly either by using stirrups beyond the supports or using forged headed bars, then the enhanced bond strength that may be mobilized in that segment could suffice to fully develop the bar. In this case the bond equation is solved considering that the available anchorage length provides for zero slip in the end – usually these are cases where pure shear failure has been observed, provided there is no local failure under the hook or head to pre-empt the development.

4 Examples from the Application of the Algorithm

To illustrate the application of the proposed methodology, two examples have been considered, to illustrate the suggested procedure. The first beam is specimen S_0 from the study of Islam et al.1998. The second specimen is $PLS300$ from the study of Quach 2016.

Specimen dimensions and loading setup for the two examples considered are shown in Fig. 6. The moment-tension steel strain relationship calculated from flexural analysis using Response2000 (Bentz and Collins 1998) of the critical section is depicted in Fig. 7. The peak bond strength was taken as $1.25\sqrt{f_c'}$ on account of the absence of confinement of the shear span.

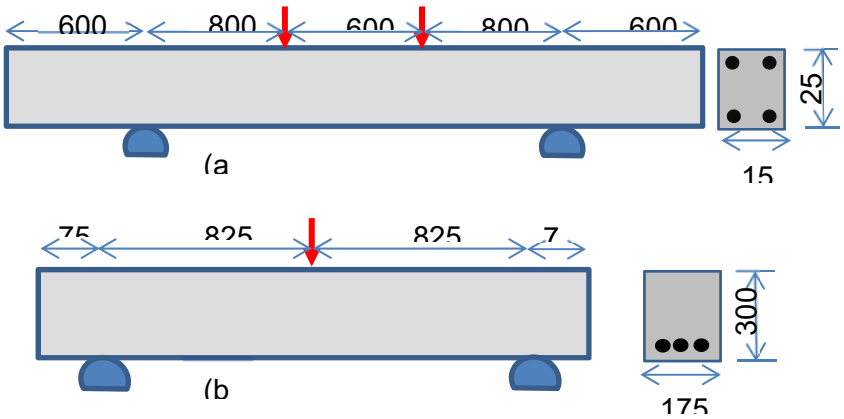

f_c'=26.6 MPa	f_y=350 MPa
D_b=20mm	c=33mm
f_b=6 MPa	s_1=0.1mm; s_2=0.25mm
f_c'=40 MPa	f_y=573 MPa
D_b=10mm	c=31mm
f_b=8 MPa	s_1=0.6mm; s_2=2.4mm

Figure 6b: Details of (a) Specimen S0 (Islam et al. 1998) and (b) Specimen PLS300 (Quach

Discussion of Analysis Results: A moment-curvature analysis was conducted for the critical cross section (section under the point load) of the two specimens, and the resulting strains in the tension reinforcement were calculated (see plots of moment strain relationships in Fig. 7(a) and (7b) for the two specimens, respectively). Furthermore, the anticipated shear strengths were calculated using the models listed in Table 1. The results are given in the following:

Table 2: Calculated shear strength values for specimens considered in the study (values in kN)

	Experiment	ACI	Collins	Cladera	Frosch	Li	Park	Reineck
S0	47.5	25.9	28.6	35.31	30	28.14	59.77	31.75
PLS300	47.7	48.5	51.23	33.6	27.15	30	43.6	32.05

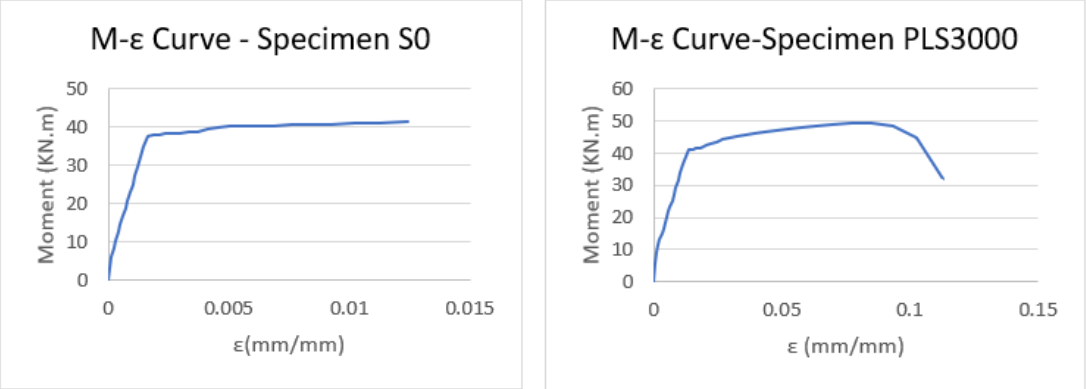

Figure 7: Calculated Moment – Tension Steel Strain relationship at the critical crack

Specimen S0: In applying the algorithm described in the preceding it was found that the first crack in the beam occurs at maximum moment of $2.36\ KN.m$ ($\varepsilon_{cr} = 0.00007$, assuming the modulus of elasticity $E_c = 4500\sqrt{26.6MPa} = 23.2\ GPa$) under the point load (this is the starting point in the x axis). Adjacent to the crack, the flexural theory is not valid and the disturbed length (l_{D1}) is estimated using the bond equation (Eq. 7, 8, and 9). With increasing strain at the critical section (under the point load) in every step, the disturbed length is calculated and the possibility of the creation of a new crack is checked (Eq. 10 and 11). In this example, the second crack happens at ε = 0.0002 outside the disturbed length of $l_{D1} = 115.83\ mm$ at $x_{cr2} = 554.01mm$ when the maximum moment is *7.67MPa*. By further increasing the strain in tension reinforcement, at ε = 0.0003, two different disturbed regions are created; $0\ to\ x_{cr2} = 554.01mm$ and $x_{cr2}\ to\ l_{D2} = 974.75mm$. In this example, after calculation of l_{D2}, it is evident that disturbed region extends beyond the support and therefore the entire length from x_{cr2} to the end of the bar length is behaving as an anchorage and the anchorage solution is implemented (Tastani and Pantazopoulou 2013a, 2013b). With further investigation of possibility of crack inside second disturbed region and increasing the strain up to ε = 0.0007 no new crack can be found. This is the stage of stabilization of cracks. At this stage the bar slip reaches the elastic bond limit ($s(x) = S_1 = 0.1mm$) at the location of the first crack ($x = 0$). For the sake of simplicity of the mathematical problem, at this stage, the entire anchorage length from the critical section to the end of the bar will be treated as an anchorage. At the strain ε = 0.000775, solving the anchorage solution for entire length ($L_b = 1400$), the bar exceeds the elastic bond limit ($s(x) > S_1 = 0.1mm$). In this stage bond plasticisation begins. By further increasing of the strain, length of l_p , where the slip at the critical section (at the start of the anchorage solution) of the bar, exceeds S_2, is found to mark the onset of debonding. From the calculations, this occurs at a bar strain of $\varepsilon_s = 0.0016$ in the critical section corresponding to a bar stress of 320MPa; from Fig. 7a, the moment at the center of the span is equal to *37 kN.m* (at a shear force = $V_c = 46.25\ KN$). Beyond attainment of the limiting slip, debonding begins from the loading point towards the support (manifested by splitting along the cover), which limits the load carrying capacity of the beam, leading to failure. The shear force sustained according to the experimental report was 47.5 KN, which is very close to the calculated value. Note that this value does not correlate with the estimates obtained from the six candidate models of C445 (Table 1) as listed in Table 2. Distributions of strains as debonding propagates from the critical section towards the end of the available bonded length are given in Figure 8.

Specimen PLS300: Applying the same algorithm to the second example, it was found that the first crack occurs at maximum moment of $4.98\ KN.m$ ($\varepsilon_{cr} = 0.000067$, assuming the modulus of elasticity $E_c = 4500\sqrt{40MPa} = 28.5\ GPa$) under the point load. Adjacent to the crack, the associated disturbed region l_{D1} is calculated (Eq. 7, 8, and 9) and the distribution of the strain in the tension bar will be estimated using Eq. 6. With increasing strain at the critical section (under the point load) in every step, at $\varepsilon = 0.001$, a disturbed length of $l_{D1} = 746.38mm$ is found and using Eq. 10 and 11, the second crack will be found inside the disturbed region at $x_{cr2} = 432.90mm$. By further increasing of the strain in tension reinforcement, at $\varepsilon_s = 0.002$, the second disturbed region, $l_{D2} = 661.62mm$, will be created and it is evident that the disturbed region extends beyond the support and therefore the entire length from x_{cr2} to the end of the bar length is behaving as an anchorage and the anchorage solution is implemented. With further investigation of

possibility of crack inside second disturbed region and increasing the strain up to ε = 0.0025 no new crack could be found. This is the stage of stabilization of cracks. At this stage the bar slip reaches the elastic bond limit ($s(x) = S_1 = 0.1mm$) at the location of the first crack ($x = 0$). For the sake of simplicity of the mathematical problem, at this stage, the entire anchorage length from the critical section to the end of the anchorage, $L_b = 1004mm$, will be treated as an anchorage. From the anchorage solution, at the strain ε = 0.003175, solving for the entire anchorage length ($L_b = 1004mm$), the bar exceeds the elastic bond limit ($s(x) > S_1 = 0.1mm$). In this stage bond plasticisation occurs and the length of l_p over which slip at the critical section (at the start of the anchorage solution) of the bar exceeds S_2, is found to mark the onset of debonding. Based on the calculations, this occurs at a bar strain in the critical section, of $\varepsilon_s = 0.011$ corresponding to the moment at the center of the span equal to *37 kN-m* (at a shear force = $V_c = 44.85\ KN$). Beyond the attainment of the limiting slip, debonding begins from the loading point towards the support (manifested by splitting along the cover), which limits the load carrying capacity of the beam, leading to failure. The shear force sustained according to the experimental report was 47.7 KN, which is very close to the calculated value.

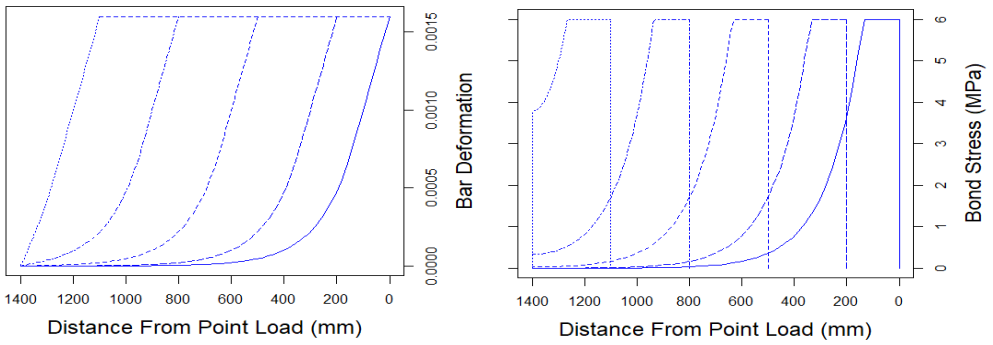

Figure 8: Distributions of bar strain and bond stress for beam S0 as debonding propagates from the critical section towards the end of the available bonded length

5 CONCLUSION

In the present paper an alternative interpretation of shear failure in beams containing no transverse reinforcement was pursued. It was shown that owing to the limited fracture energy of the bond-slip curve, debonding begins once the maximum sustainable slip is exceeded at the critical sections of flexural beams. Beyond that point, strain penetration follows, spreading from the section of maximum moment (under the point load) toward the end of the anchorage on a beam. The behavior of the tension steel reinforcement is therefore governed by the bond equations after stabilization of cracking, and not by flexural equations. Once this event occurs splitting governs the bar anchorage whereas beam failure occurs when the residual bonded length can no longer equilibrate the bar force required for flexure. In order to calculate the shear strength of a beam in a manner consistent with above definition, the solution of two different examples was provided. The results show good agreement with the experimental results and highlight the limitations of the proposals for shear strength (V_c) of beams with no shear reinforcement which are oblivious to bond and its implications. It is noteworthy to mention that there is a need for simplification as prerequisite to its application in practical design, and the necessary further corroboration with the Shear Database.

Acknowledgements

This research has been conducted at York University, partially sponsored by NSERC DG – 2016- 05324.

References

ACI Committee 318. 2014. *Building Code Requirements for Structural Concrete (ACI 318-14) and Commentary, (ACI 318R-14),* American Concrete Institute, Farmington Hills, MI, USA.

Bazant, Z. P., and Planas, J. 1997. “Fracture and Size Effect in Concrete and Other Quasibrittle Materials”,***16****, CRC Press, Boca-Raton, Fl, USA.*

Bažant, Z. P. 1999. “Size Effect on Structural Strength: A Review.” *Archive of Applied Mechanics (Ingenieur Archiv)* **69** (9–10): 703–25. doi:10.1007/s004190050252.

Belarbi, A., Kuchma, D.A., and Sanders D.H. 2017. “Proposals for New One-Way Shear Equations for the 318 Building Code.” *Concrete International* **39** (9): 29–32.

Bentz, E.C., and Collins, M.P. 2017. “Updating the ACI Shear Design Provisions.” *Concrete International* **39** (9): 33–38.

Bentz, Evan C., and Michael P. Collins. *Response-2000: Reinforced Concrete Sectional Analysis using the Modified Compression Field Theory*. 1998.

Cladera, A., and A. R. Marí. 2004. “Shear Design Procedure for Reinforced Normal and High-Strength Concrete Beams Using Artificial Neural Networks. Part II: Beams with Stirrups.” *Engineering Structures* **26** (7): 927–36. doi:10.1016/j.engstruct.2004.02.011.

Cladera, A., Marí A., Bairán J.-M., Oller E., and Ribas, C. 2017. “One-Way Shear Design Method Based on a Multi-Action Model.” *Concrete International* **39** (9): 40–46.

Collins, M.P., and Kuchma D. A. 1999. “How Safe Are Our Large Lightly Reinforce Concrete Beams.” *ACI Structural Journal* **96** (4): 482–90.

Grégoire D., Rojas-Solano L. B., Pijaudier-Cabot G. 2013. “Failure and Size Effect for Notched and Unnotched Concrete Beams.” *International Journal for Numerical and Analytical Methods in Geomechanics* **32** (March 2007): 189–213. doi:10.1002/nag.

Daluga, Derek, Kaylor McCain, Matthew Murray, and Santiago Pujol. 2017. “Effect of Geometric Scaling on Shear Strength of Reinforced Concrete Beams with Stirrups.” *ACI Structural Journal* **114** (6): 1397–1406. doi:10.14359/51700947.

Frosch, R.J., Yu, Q., Cusatis G., and Bažant, Z. P. 2017. “A Unified Approach to Shear Design.”*, Concrete International* **39** (9): 47–52.

fib Bulletin 72 (2014). "Bond and anchorage of embedded reinforcement", ISBN: 978-2-88394-112-0, Federation International du Beton, Lausanne, http://www.fib-international.org.

fib Model Code 2010 for Concrete Structures (2013). http://www.fib-international.org/fib-model-code-2010

Islam, M.S., H.J. Pam, and A.K.H. Kwan. 1998. “Shear Capacity of High-Strength Concrete Beams with Their Point of Inflection within the Shear Span.” *ICE: Structures and Buildings.* **128**: 91–99.

Kani, G. N. J. 1967. “How Safe Are Our Large Reinforced Concrete Beams?” *ACI Journal Proceedings* **64** (3). doi:10.14359/7549.

Karihaloo, B.L., Abdalla H.M., and Xiao Q. Z. 2003. “Size Effect in Concrete Beams.” *Engineering Fracture Mechanics* **70** (7–8): 979–93. doi:10.1016/S0013-7944(02)00161-3.

Kirane, Kedar, Konjengbam Darunkumar Singh, and Zdeněk P. Bažant. 2016. “Size Effect in Torsional Strength of Plain and Reinforced Concrete.” *ACI Structural Journal* **113** (6): 1253–62.

Li, YA, TTC Hsu, SJ Hwang - Concrete International, and undefined 2017. 2018. “Shear Strength of Prestressed and Nonprestressed Concrete Beams.” *Concrete.org*.

Megalooikonomou, K. G., S. P. Tastani, and S. J. Pantazopoulou. 2018. “Effect of Yield Penetration on Column Plastic Hinge Length.” *Engineering Structures* **156**: 161–74, Elsevier.

Ozbolt, J., and and R. Eligehausen. 1995. “SIZE EFFECT IN CONCRETE AND REINFORCED CONCRETE STRUCTURES.” *Structures, Fracture Mechanics of Concrete*, 1529–38.

Park, Hong-Gun, and Kyoung-Kyu Choi. 2017. “Unified Shear Design Method of Concrete Beams Based on Compression Zone Failure Mechanism.” *Concrete International* **39** (9): 59–63.

Quach, Phillip T. "Understanding and safely predicting the shear response of large-scale reinforced

concrete structures." PhD diss., University of Toronto (Canada), 2016.

Reineck, Karl-Heinz. 2017. “Proposal for ACI 318 Shear Design.” *Concrete International* **39** (9): 65–70.

Reineck, K.-H., Kuchma, D.A., Kim K.S., and Marx S. 2003. “Shear Database for Reinforced Concrete Members without Shear Reinforcement.” *ACI Structural Journal* **100** (2): 240–49.

Tastani, S. P., and J. Pantazopoulou. 2013a. “Yield Penetration in Seismically Loaded Anchorages: Effects on Member Deformation Capacity.” *Earthquake and Structures* **5** (5): 527–52.

Tastani, S P, and S J Pantazopoulou. 2013b. “Reinforcement and Concrete Bond: State Determination along the Development Length.” *Journal of Structural Engineering (United States)* **139** (9): 1567–81.

Taylor, Howard PJ. "Shear strength of large beams." Journal of the Structural Division 98, no. Proc Paper 9329 (1972).